Dalton Transactions

RSC Publishing

PAPER

View Article Online
View Journal

Cite this: DOI: 10.1039/c3dt52578c

Synthesis, structure and dynamics of NHC-based palladium macrocycles†

Rhiann E. Andrew and Adrian B. Chaplin*

A series of macrocyclic CNC pincer pro-ligands based on bis(imidazolium)lutidine salts with octa-, deca- and dodecamethylene spacers have been prepared and their coordination chemistry investigated. Using a Ag_2O based transmetallation strategy, cationic palladium(II) chloride complexes $[PdCl\{CNC–(CH_2)_n\}][BAr^F_4]$ (n = 8, 10, 12; Ar^F = 3,5-$C_6H_3(CF_3)_2$) were prepared and fully characterised in solution, by NMR spectroscopy and ESI-MS, and in the solid-state, by X-ray crystallography. The smaller macrocyclic complexes (n = 8 and 10) exhibit dynamic behaviour in solution, involving ring flipping of the alkyl spacer across the Pd–Cl bond, which was interrogated by variable temperature NMR spectroscopy. In the solid-state, distorted coordination geometries are observed with the spacer skewed to one side of the Pd–Cl bond. In contrast, a static C_2 symmetric structure is observed for the dodecamethylene based macrocycle. For comparison, palladium(II) fluoride analogues $[PdF\{CNC–(CH_2)_n\}][BAr^F_4]$ (n = 8, 10, 12) were also prepared and their solution and solid-state structures contrasted with those of the chlorides. Notably, these complexes exhibit very low frequency ^{19}F chemical shifts (*ca.* −400 ppm) and the presence of C–H···F interactions ($^{2h}J_{FC}$ coupling observed by ^{13}C NMR spectroscopy). The dynamic behaviour of the fluoride complexes is largely consistent with the smaller ancillary ligand; $[PdF\{CNC–(CH_2)_8\}][BAr^F_4]$ exceptionally shows C_{2v} time averaged symmetry in solution at room temperature (CD_2Cl_2, 500 MHz) as a consequence of dual fluxional processes of the pincer backbone and alkyl spacer.

Received 18th September 2013,
Accepted 28th October 2013

DOI: 10.1039/c3dt52578c

www.rsc.org/dalton

Introduction

N-heterocyclic carbenes (NHCs) have quickly emerged as a powerful class of carbon-based ligand in organometallic chemistry and catalysis.[1] With generally stronger σ-donating characteristics and orthogonal steric profiles to widely used phosphine ligands, NHCs are rapidly being established as ligands of choice for many transition metal catalysed reactions. Aided by simple and efficient synthetic protocols, intricate polydentate ligand topologies can be readily constructed based on NHC donors.[2,3] Building on the flourishing chemistry of phosphine-based pincer complexes,[4] analogous NHC-based tridentate architectures have received considerable attention in particular.[2,5] Archetypical NHC pincer ligands are derived from bis(imidazol-2-ylidene)-benzene, pyridine, xylene or lutidine frameworks (Fig. 1) and the coordination chemistry of these CNC and CCC pincer ligands has been explored for a variety of late transition metals.[2,5,6] Notably, palladium CNC based complexes have been thoroughly investigated, following seminal work by Crabtree and Piers who demonstrated the application of these species in cross coupling reactions.[7–14]

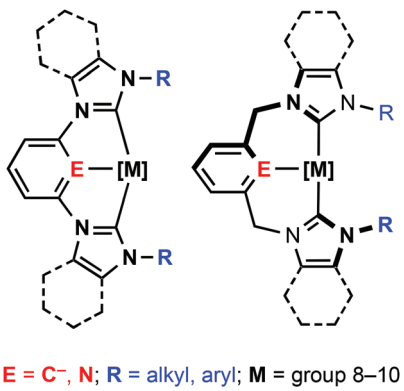

E = C⁻, N; R = alkyl, aryl; M = group 8–10

Fig. 1 NHC-based pincer architectures.

The substitution geometries of NHC pincers are well suited to the construction of macrocycles. Principally based on lutidine and xylene backbones, tridentate macrocycles find notable application in supramolecular chemistry; exploiting chemistry of the coordinated metal centre for molecular recognition[15] and the construction of interlocked catenane and rotaxane systems.[16] The vast majority of known CNC and CCC

Department of Chemistry, University of Warwick, Gibbet Hill Road, Coventry CV4 7AL, UK. E-mail: a.b.chaplin@warwick.ac.uk

†Electronic supplementary information (ESI) available. CCDC 961289–961294. For ESI and crystallographic data in CIF or other electronic format see DOI: 10.1039/c3dt52578c

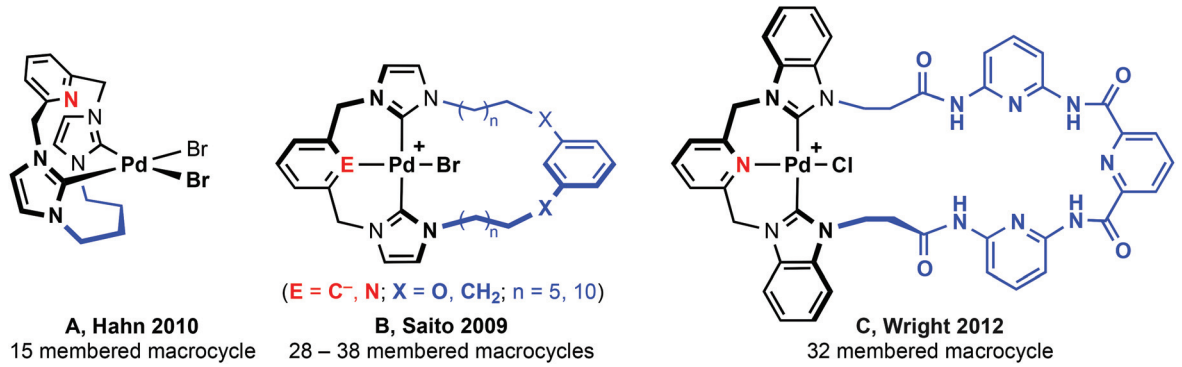

Fig. 2 NHC-based macrocyclic complexes.

based pincer complexes feature ligands bearing simple alkyl (*i.e.* Me, ^{n}Bu, ^{t}Bu, Ad) and aryl (*e.g.* Mes, Dipp) groups. Despite facile synthetic procedures to macrocyclic imidazolium pro-ligands,[17] there are very few examples of tridentate NHC-based macrocyclic complexes. Macrocyclic complexes that have been reported are limited to small (*e.g.* **A**, 15 membered, Fig. 2)[18,19] or very large ring sizes (**B** and **C**; 28–38 membered).[20,21] Of these systems, tridentate coordination of the macrocycle was observed within **B** and **C**, although not in **A**; the smaller 15 membered ring adopting a bidentate cyclophane geometry[2,22] with no pyridine coordination as a consequence of the short butamethylene spacer. Although showing significantly lower catalytic activity than related non-macrocyclic variants,[7,10,13,14] both xylene and lutidine based **B**, promote C–C bond coupling reactions.[20]

Motivated by the possibility for exploiting their unique steric profile in organometallic chemistry and potential applications as building blocks in interlocking architectures, in this communication we present the synthesis of a range of medium sized (19–23 membered) macrocyclic pro-ligands consisting of bis(imidazolium)lutidine salts with octa-, deca- and dodecamethylene spacers. The coordination chemistry of the corresponding CNC pincer ligands with palladium is detailed, particularly focusing on the effect of the aliphatic chain and ancillary ligands on the structure and dynamics of the resulting macrocyclic complexes, as probed by variable temperature NMR spectroscopy and X-ray diffraction.

Results and discussion

The target macrocyclic pro-ligands [CNC–$(CH_2)_n$]·2(HBr) (n = 8, **2a**; 10, **2b**; 12, **2c**) were prepared as bromide salts using a straightforward two-step synthesis, involving alkylation of 2,6-bis(bromomethyl)pyridine with bis(imidazole)alkanes **1** in dioxane (Scheme 1). All three intermediate bis-imidazoles (n = 8, 10, 12) were readily prepared following minor adaptions to literature procedures employing commercially available alkyl dibromides.[23] The overall synthetic route readily afforded gram scale quantities of **2** in high purity following recrystallisation from acetonitrile–diethyl ether (19–32% overall yields). The

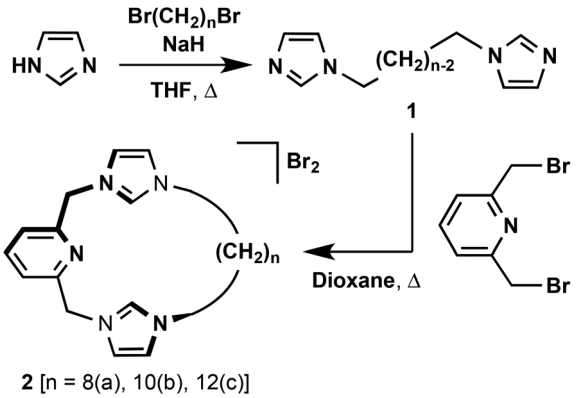

Scheme 1 Preparation of pro-ligands **2**.

salts are notably hygroscopic and best stored and manipulated under a dry inert atmosphere.

The structures of **2** were confirmed by a combination of NMR spectroscopy and ESI-MS, with the latter being particularly diagnostic. Strong dication parent ion signals are observed for each compound: **2a**, 175.6207 (calc. 175.6206) m/z; **2b**, 189.6361 (calc. 189.6362) m/z; **2c**, 203.6521 (calc. 203.6519) m/z. The NMR spectra of **2** in CD_2Cl_2 exhibit singlet 4H resonances for the methylene bridge at *ca.* 5.8 ppm, with characteristic ^{1}H and ^{13}C signals of the pre-carbenic centre at *ca.* 10.7 and 138 ppm, respectively. The remaining features of the spectroscopic data fully corroborate the structures of **2** and are otherwise unremarkable. Satisfactory microanalysis was obtained for all the macrocycles, and the structure of **2b** was further confirmed by X-ray crystallography (ESI†).

Typically, coordination of CNC pincers to palladium has been achieved through reaction of the corresponding imidazolium pro-ligands with $[Pd(OAc)_2]$ in DMSO at elevated temperatures.[5] With a view of developing a more general procedure for the coordination of pro-ligands **2** with transition metals, we have adapted Ag_2O based transmetallation strategies previously employed by Youngs, Danopoulos and Cavell for this initial work involving palladium.[9–11] This procedure is outlined in Scheme 2, and involves reactions of **2** with Ag_2O and $Na[BAr^F_4]$ (Ar^F = 3,5-$C_6H_3(CF_3)_2$) in CH_2Cl_2, followed by

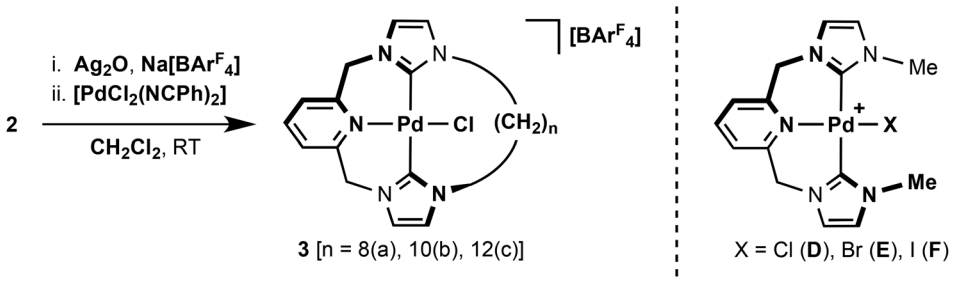

Scheme 2 Preparation of **3**.

subsequent addition of $[PdCl_2(NCPh)_2]$ as a source of palladium(II) halide – all carried out at room temperature. Using this convenient and mild procedure, macrocyclic palladium complexes $[PdCl\{CNC–(CH_2)_n\}][BAr^F_4]$ (n = 8, **3a**; 10, **3b**; 12, **3c**) were prepared with moderate-to-good isolated yields of 31% (n = 8), 55% (n = 10) and 58% (n = 12), following purification on silica and recrystallisation. $[PdCl_2(NCMe)_2]$ can also be used as the palladium(II) halide source, but gave no significant improvements in yield. Complexes **3** are air stable both in solution and the solid state; dissolving readily in CH_2Cl_2, $CHCl_3$, Et_2O and MeCN. No attempts were made to isolate the corresponding intermediate silver complexes, although we note that the incorporation of the $[BAr^F_4]^-$ anion appears to plays an import role in solubilising these species throughout the procedure.

The palladium complexes **3** were fully characterised by NMR spectroscopy, ESI-MS and elemental analysis. Coordination of the ligand was confirmed through the presence of strong parent ion peaks with the expected isotope distributions in mass spectra [**3a**, 490.0993 (calc. 490.0989) m/z; **3b**, 518.1308 (calc. 518.1303) m/z; **3c**, 546.1616 (calc. 546.1617) m/z]. ^{1}H and ^{13}C NMR spectra further corroborate the structures of the compounds, which all exhibit approximate C_2 symmetry in solution at room temperature ($CDCl_3$ and CD_2Cl_2, 400 or 500 MHz). The binding of the ligand through carbene donors is established by the absence of the distinctive high frequency imidazolium proton resonances of **2** and significant ^{13}C shifts of the carbene centre from *ca.* 138 to 163 ppm. These carbene resonances differ only marginally within the series of complexes, although a positive correlation with increasing frequency and macrocycle size is noted, *i.e.* 162.4 (**3a**), 163.3 (**3b**), 164.5 (**3c**) ppm. All values are in good agreement with that observed for the non-macrocyclic analogue $[PdCl\{CNC–Me\}]^+$ **D** (164 ppm, Scheme 2).[13] Complexes **3** show interesting dynamic behaviour in solution and these features are discussed below in detail.

Crystal structures of all three palladium macrocycles were obtained, revealing significant structural differences between the complexes (Fig. 3 and Table 1). Tridentate coordination of the macrocyclic ligand is observed for each complex, with the pincer moiety adopting a characteristic twisted pseudo C_2 conformation, where the pyridine (*ca.* 40°) and imidazolylidene rings are angled out of the coordination plane as a consequence of the methylene bridges.[8–10,13] Associated Pd1–N1 (*ca.* 2.1 Å), Pd1–C (*ca.* 2.0 Å) and Pd1–Cl1 (*ca.* 2.3 Å) distances closely match those found in other related palladium CNC pincer complexes, as exemplified by comparison to **D** (Table 1).[13] The principle differences between the structures are manifested in the conformation of the alkyl spacer, which is skewed to one side of the Pd–Cl bond for the shorter spacers (n = 8 and 10) as a consequence of the steric interactions between the spacer and the chloride ligand. This interaction distinctly leads to distortions of the metal coordination geometry which are most pronounced for **3a**, with C7–Pd1–C11 and especially N1–Pd1–Cl1 angles deviating dramatically from 180° [168.82(7) and 163.39(4)°]. With the largest dodecamethylene spacer, **3c** adopts an overall pseudo C_2 geometry, with the coordinated chloride ligand fully enclosed within the macrocycle cavity; the C7–Pd1–C11 and N1–Pd1–Cl1 angles are essentially linear [172.8(6) and 176.2(3)°] as observed for non-macrocyclic **D** [173.60(7) and 178.19(3)°].[13] Related palladium chloride CNC pincer complexes bearing bulky ^{t}Bu, Mes and Dipp substituents retain N–Pd–Cl bond angles of effectively 180°.[8–10] Distortion from linearity is uncommon within known palladium(II) square planar complexes (following inspection of CSD metrics), although complexes with angles down to 150° are known.[24]

To investigate the apparent inconsistency between the solution (C_2 symmetry) and solid-state (C_1 symmetry) structures of **3a** and **3b**, we turned to variable temperature NMR measurements. The fluxional behaviour of CNC based pincer complexes $[PdX\{CNC–Me\}]^+$ **D–F** (Scheme 2) has previously been investigated in detail by Crabtree and co-workers.[12,14] These complexes undergo atropisomerisation between left and right-handed C_2 conformations with a free energy barrier of 60.0 kJ mol^{-1} for [**D**]Cl (CD_2Cl_2, T_c = 303 K for the methylene bridge protons).[25] The rate of this process is highly dependent on the halide–anion combination. Increased activation barriers are observed for complexes containing the weakly coordinating OTs^- anion ([**D**]OTs, $\Delta G^{\ddagger}(CDCl_3)$ = 66.0 kJ mol^{-1}) and along the series: [**F**]I, [**E**]Br, [**D**]Cl [$\Delta G^{\ddagger}(CDCl_3)$ = 41.9, 52.9 and 59.3 kJ mol^{-1}]. On the basis of these observations and supporting computational work, a two-step interconversion mechanism involving dissociation of the pyridine group and coordination of the counter anion was proposed. Atropisomerisation ($\Delta G^{\ddagger}(CDCl_3)$ = 57–59 kJ mol^{-1}) is also observed in the macrocyclic complexes [**B**]Br (Fig. 2, E = N) although only very small changes in barrier height are observed in comparison to

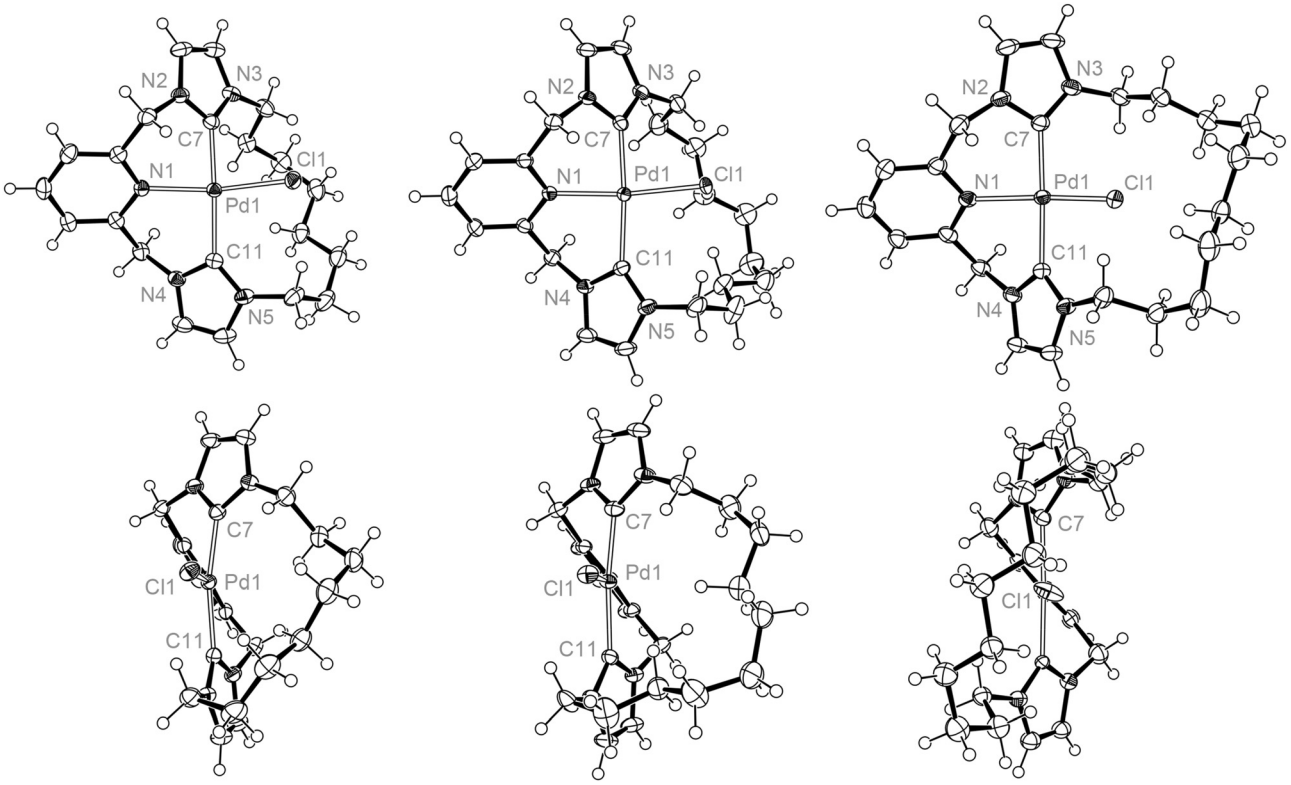

Fig. 3 Solid-state structures of **3a**, **3b** and **3c** viewed perpendicular (top) and along (bottom) Pd1–N1 bond vectors. Thermal ellipsoids drawn at 50%; minor disordered component (alkyl spacer) in **3b**, anions and solvent molecules omitted for clarity. Selected structural metrics are listed in Table 1.

Table 1 Selected bond lengths (Å) and angles (°) for **3** and **D** (ref. 13)[a]

	3a	3b	3c	D
Pd1–N1	2.087(2)	2.080(2)	2.077(10)	2.068(1)
Pd1–Cl1	2.3051(5)	2.3217(5)	2.287(4)	2.2978(5)
Pd1–C7	1.983(2)	2.004(2)	2.056(13)	2.026(2)
Pd1–C11	2.073(2)	2.078(2)	2.036(12)	2.029(2)
N1–Pd1–Cl1	163.39(4)	166.29(5)	176.2(3)	178.19(3)
C7–Pd1–C11	168.82(7)	171.93(8)	172.8(6)	173.60(7)
C7–Pd1–Cl1	86.19(5)	87.76(6)	95.9(4)	93.15(5)
C11–Pd1–Cl1	98.40(5)	98.22(6)	91.1(4)	93.21(5)
lspl(NHC) ∠lspl(NHC′)	70.72(8)	76.88(9)	81.0(5)	85.08(7)[b]
lspl(py) ∠lspl(coord.)	33.07(6)	39.14(7)	42.5(4)	41.83(5)[b]

[a] lspl(atoms) denotes the least squares plane through the indicated group of atoms; coord. refers to Pd1, C7, C11 and N1. [b] Recalculated using CIF matrix from ref. 13.

the directly related ^{n}Bu substituted analogue [PdBr{CNC–^{n}Bu}]-Br ($\Delta G^{\ddagger}(CDCl_3)$ = 57.4 kJ mol^{-1}) – indicating no significant macrocyclic effect.[20] Remarkably, no dynamic behaviour of the pincer coordination geometry is observed for **3** with the methylene bridge protons diastereotopic in CD_2Cl_2 solution (500 MHz) up to 308 K (*i.e.* $\Delta G^{\ddagger} \gg 62$ kJ mol^{-1}). This is consistent with the non-coordinating nature of the $[BAr^F_4]^-$ anion[26] and the calculated gas-phase barrier of **D** of 73.2 kJ mol^{-1}.[12]

In agreement with the solid-state structure, **3c** retains C_2 symmetry from 200–298 K in CD_2Cl_2 solution (500 MHz), further confirming the good fit of the coordinated chloride ligand within the cavity of the macrocyclic ligand. For complexes **3a** and **3b**, variable temperature NMR experiments demonstrate ring flipping of the macrocycle across the palladium chloride bond. This fluxional process mediates an atropisomerisation between skewed C_1 symmetric confirmations observed in the solid-state (Fig. 3) and leads to the time averaged C_2 symmetry in solution at room temperature. For **3a**, the slow exchange limit for this process is reached at 200 K in CD_2Cl_2 (500 MHz), with the ^{1}H NMR spectrum showing three pyridine and four imidazolylidene resonances together with pairs of diastereotopic methylene bridge (pyCH_2) and *N*-CH_2 signals (Fig. 4). Simulation[27] of the ^{1}H NMR data over the temperature range 185 to 298 K allowed rate data to be extracted for the exchange process, leading to values of $\Delta H^{\ddagger}$ = 43 ± 4 kJ mol^{-1}, $\Delta S^{\ddagger}$ = −7 ± 17 J mol^{-1} K^{-1} and $\Delta G^{\ddagger}$(298 K) = 45 ± 9 kJ mol^{-1} following an Eyring analysis (see ESI†). In line with the longer alkyl spacer, the fluxional process in **3b** is much faster than **3a**: the exchange could not be completely frozen out, even upon cooling to 185 K, although the barrier for this process can be approximated at $\Delta G^{\ddagger}$ = 37 kJ mol^{-1} from signal coalescence at low temperature.[28]

To further investigate the dynamics of the macrocyclic ligands, metathesis of the chloride ligand with the smaller fluoride ligand was targeted. This was achieved by reactions of **3** with excess AgF in acetonitrile to afford the palladium(II) fluoride complexes [PdF{CNC–$(CH_2)_n$}][BAr^F_4] (*n* = 8, **4a**; 10, **4b**; 12, **4c**) with good to moderate isolated yields of 45–88%

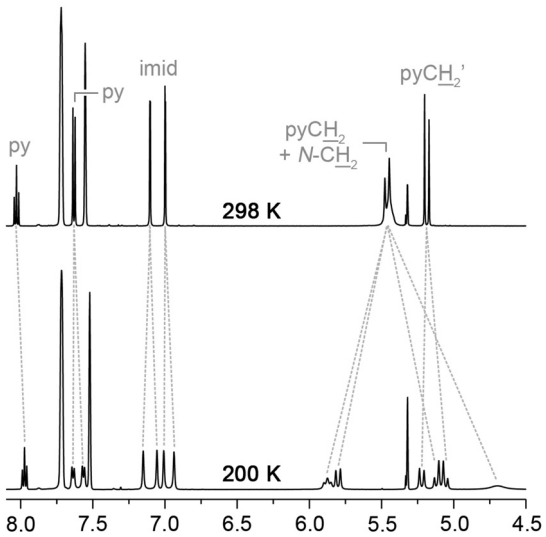

Fig. 4 Selected ^{1}H NMR spectra of **3a** (CD_2Cl_2, 500 MHz).

(Scheme 3). Unlike their palladium(II) chloride analogues, the fluorides are markedly water sensitive and degrade readily on silica. Facile loss of the fluoride ligand is also apparent by ESI-MS and only fragment ion derivatives can be observed. Although many examples of palladium fluoride complexes containing phosphine and nitrogen based donor ligands are known,[29] to the best of our knowledge no NHC based analogues have been reported. The formation of **4** are readily corroborated by ^{1}H, ^{13}C and ^{19}F NMR spectroscopy and elemental analysis. The coordinated carbene centres are observed as broad singlets at *ca.* 165 ppm by ^{13}C NMR spectroscopy to slightly higher frequency than observed in **3**, while ^{19}F NMR spectra reveal characteristically low frequency Pd(II) fluoride resonances at *ca.* −400 ppm. ^{19}F chemical shifts of this magnitude are uncommon,[30] although notably the palladium PNP pincer **G** (Scheme 3) has a ^{19}F NMR shift of −414.3 ppm for the coordinated fluoride ligand.[31]

Like its chloride analogue, temperature invariant ^{1}H NMR spectra of **4c** demonstrate the adoption of C_2 symmetry in solution. For the smaller **4b**, a very low energy fluxional process can be detected only by cooling to 185 K, where the onset of coalescence is noted for one of the *N*-CH_2 resonances. In comparison to **3b**, the interconversion barrier for **4b** must be considerably less as at 185 K the slow exchange limit is essentially reached for all signals of **3b**. Given the large $\Delta\nu$ possible for the *N*-CH_2 shifts it is difficult to approximate the barrier, although we estimate a value of $\Delta G^{\ddagger} \leq 34$ kJ mol^{-1} (based on $\Delta\nu$ = 600 Hz from **3a**). The solid-state structure of **4b** shows a more symmetric structure than **3b** (Fig. 5), with the N1–Pd1–F1 angle approaching 180° [175.77(7) *cf.* 166.29(5)° for **3b**], although meaningful conclusions from this observation are difficult due to crystal packing effects. Notably the cations in **4b** pack with relatively close Pd1–Pd1′ and Pd1–F1′ distances of 4.3357(7) and 3.866(2) Å, respectively. A further interesting feature of note is the presence of weak *N*-CH–H···F interactions, which were detected by carbon–fluorine coupling for both **4b** and **4c** ($^{2h}J_{FC}$ = 6 Hz, 298 K). These $^{2h}J_{FC}$ values and the corresponding interatomic distances observed in

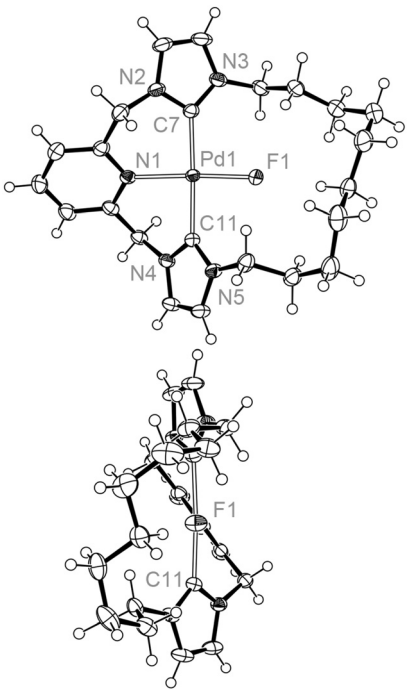

Fig. 5 Solid-state structures of **4b** viewed perpendicular (top) and along (bottom) the Pd1–N1 bond vector. Thermal ellipsoids drawn at 50%, anion omitted for clarity. Selected bond lengths (Å) and angles (°): Pd1–N1, 2.035(2); Pd1–F1, 1.9588(13); Pd1–C7, 2.018(2); Pd1–C11, 1.999(2); N1–Pd1–F, 175.77(7); C7–Pd1–C11, 175.66(10); C7–Pd1–F1, 92.96(8); C11–Pd1–F1, 88.99(7); lspl(NHC) ∠lspl(NHC′), 73.2(1); lspl(py) ∠lspl(coord.), 36.52(8).

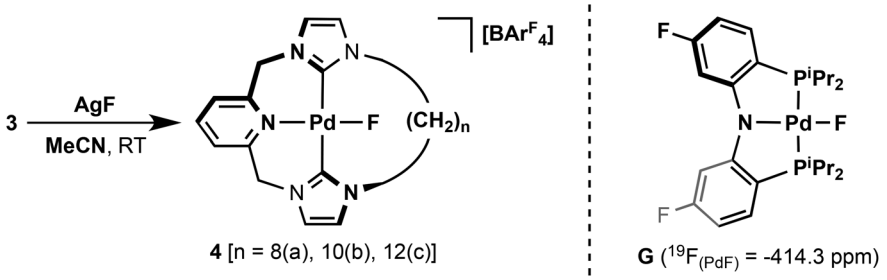

Scheme 3 Preparation of **4**.

solid-state structure of **4b** [C···F = 2.968(3), 3.146(3) Å], are fully consistent with other C–H···F interactions reported in the literature.[32]

In solution, **4a** is highly fluxional. At 298 K in CD_2Cl_2 (500 MHz), C_{2v} symmetry is observed indicating an atropisomerisation mechanism involving dynamics of both the pincer and octamethylene spacer. Upon cooling the sample to 225 K onset of decoalescence of the methylene bridge and *N*-CH_2 protons was observed, while those of the imidazolylidene remained relatively sharp. Further cooling to 185 K led to broadening of the later signals, although the slow exchange limit was not reached (precluding accurate simulation). These observations support a dual fluxional process involving low energy flipping of the octenyl linker ($\Delta G^{\ddagger} \leq 34$ kJ mol^{-1}) and higher energy pincer twisting ($\Delta G^{\ddagger} \sim 43$ kJ mol^{-1}). The latter process is characteristic of **D–F**, with the approximate barrier height of 43 kJ mol^{-1} being broadly similar to that calculated for dicationic $[Pd\{CNC–Me\}]^{2+}$ ($\Delta G^{\ddagger} = 47.8$ kJ mol^{-1})[12] and suggestive of fluoride ligand dissociation (promoted by macrocycle induced steric pressure). Although we could obtain a solid-state structure of **4a**, somewhat inline with its highly fluxional solution characteristics, it has two crystallography independent cations both with extensively disordered macrocycle geometries (see ESI†). However, what is clear from the structure is that the octamethylene group is skewed to one side of the palladium(II) fluoride bond (as with **3a** and **3b**) and the N–Pd–F angle deviates from linearity (*ca.* 172°). The shorter macrocycle linker also results in further close C–H···F interactions, with coupling at 1,8- ($^{2h}J_{FC} = 14$ Hz) and 4,5- ($^{2h}J_{FC} = 6$ Hz) positions along the octamethylene group resolved by ^{13}C NMR spectroscopy.

Summary

A series of macrocyclic CNC pincer pro-ligands have been prepared incorporating simple alkyl spacers, resulting in 19, 21 and 23 membered ring systems (**2**). The coordination chemistry of these pro-ligands has been explored, and a series of cationic palladium(II) chloride (**3**) and fluoride (**4**) complexes have been synthesised and fully characterised in solution and the solid-state. The larger macrocyclic complexes, containing dodecamethylene spacers, exhibit static C_2 symmetric structures with the coordinated halogen ligands lying within the macrocyclic cavity. As the ring size is reduced, increasing dynamic behaviour is observed in solution, with the spacer undergoing ring flipping across the palladium halogen bond, and is most pronounced with the larger chloride ancillary ligand (Table 2). The atropisomerisation of the smaller macrocyclic complexes is also manifested in their solid-state structures, with significant distortions from the expected square planar geometries and skewing of the alkyl spacers to one side of the palladium–halogen bonds observed. The dodecamethylene based CNC pincer ligands accommodate the coordinated metal–ligand moiety most readily and appear most suitable for subsequent applications in organometallic chemistry and as building blocks for interlocking architectures: the organometallic chemistry of other late transition complexes bearing this ligand is currently being explored.[33]

Table 2 Summary of the structure and dynamics of **3** and **4**

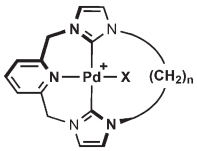

n\X	Cl	F
8	Fluxional spacer ($\Delta G^{\ddagger} = 43$ kJ mol^{-1})	Highly fluxional macrocycle
10	Fluxional spacer ($\Delta G^{\ddagger} = 37$ kJ mol^{-1})	Fluxional spacer ($\Delta G^{\ddagger} \leq 34$ kJ mol^{-1})
12	C_2 symmetric (Cl enclosed)	C_2 symmetric (F enclosed)

Experimental

General considerations

Manipulations were performed under an inert atmosphere, using Schlenk (nitrogen) and glove box (argon) techniques unless otherwise stated. Glassware was oven dried and flamed under vacuum prior to use. Anhydrous solvents (<0.005% H_2O) were purchased from ACROS or Aldrich and used as supplied: MeCN, CH_2Cl_2, $CHCl_3$, THF, 1,4-dioxane, pentane and Et_2O. CD_2Cl_2 was dried over CaH_2, vacuum-distilled and stored under an atmosphere of argon. $CDCl_3$ (for NMR characterisation of **4**) was dried over 3 Å molecular sieves, vacuum-distilled and stored over sieves. $Na[BAr^F{}_4]$[34] and $[Rh(CO)_2Cl]_2$ [35] were synthesised using literature procedures. Bis-imidazoles **1** were prepared by adaptions of literature procedures and are fully detailed in the ESI.†[23] $[PdCl_2(NCPh)_2]$, $[PdCl_2(NCMe)_2]$, Ag_2O, AgF, 2,6-bis(bromomethyl)pyridine, and dibromoalkanes are commercial products and were used without further purification. NMR spectra were recorded on Bruker DPX-400, AV-400 and DRX-500 spectrometers at 298 K unless otherwise stated. Chemical shirts are quoted in ppm and coupling constants in Hz. ESI-MS were recorded on a Bruker MaXis mass spectrometer. Microanalyses were performed at the London Metropolitan University by Stephen Boyer.

Preparation of pro-ligands (2)

General procedure. To refluxing 1,4-dioxane (150 mL), equimolar solutions of 2,6-bis(bromomethyl)pyridine and bis-imidazole **1** in THF (*ca.* 0.075 M, dried over 3 Å molecular sieves) were simultaneously added dropwise over 30 minutes. The resulting reaction mixture was refluxed for 16 hours, cooled to approx. 50 °C and the solvent removed *in vacuo*. The resulting off-white residue was extracted with MeCN (*ca.* 200 mL) with vigorous stirring. The MeCN solution was filtered, concentrated and excess Et_2O added to precipitate the product. The product was isolated by filtration and washed with excess Et_2O.

2a: following the general procedure using 2,6-bis(bromomethyl)pyridine (0.79 g, 2.98 mmol) and **1a** (0.73 g, 2.98 mmol), the product was obtained as an off-white foam. Yield: 0.47 g (31%).

^{1}H NMR (400 MHz, CD_2Cl_2) δ 10.55 (app. t, J = 2, 2H), 8.00 (app. t, J = 2, 2H), 7.82 (dd, $^3J_{HH}$ = 8.4, 7.0, 1H), 7.72 (app. d, J = 8, 2H), 7.40 (app. t, J = 2, 2H), 5.82 (s, 4H), 4.42 (t, $^3J_{HH}$ = 6.4, 4H), 1.88 (app. pentet, J = 7, 4H), 1.32–1.41 (m, 4H), 1.18–1.28 (m, 4H). **^{13}C{^{1}H} NMR** (101 MHz, CD_2Cl_2) δ 153.6, 139.5, 137.9, 124.6, 124.4, 122.1, 54.2, 50.1, 29.6, 27.5, 24.7. **ESI-MS** (CH_2Cl_2, 180 °C, 3 kV) positive ion: 175.6207 m/z, $[M]^{2+}$ (*calc.* 175.6206). **Anal.** Calcd for $C_{21}H_{29}N_5Br_2{\cdot}1.4(H_2O)$ (536.52 [511.30] g mol^{-1}): C, 47.01; H, 5.97; N, 13.05. Found: C, 47.17; H, 5.45; N, 13.01.

2b: following the general procedure using 2,6-bis(bromomethyl)pyridine (1.00 g, 3.77 mmol) and **1b** (1.03 g, 3.77 mmol), the product was obtained as a white crystalline solid. Yield: 0.71 g (35%).

^{1}H NMR (400 MHz, CD_2Cl_2) δ 10.80 (app. t, J = 2, 2H), 7.94 (app. t, J = 2, 2H), 7.82 (dd, $^3J_{HH}$ = 8.1, 7.3, 1H), 7.69 (app. d, J = 8, 2H), 7.23 (app. t, J = 2, 2H), 5.82 (s, 4H), 4.42 (t, $^3J_{HH}$ = 7.1, 4H), 1.96 (app. pentet, J = 7, 4H), 1.37–1.46 (m, 8H), 1.30–1.35 (m, 4H). **^{13}C{^{1}H} NMR** (101 MHz, CD_2Cl_2) δ 153.7, 139.6, 138.5, 124.4, 123.8, 121.9, 54, 50.5, 29.6, 27.9, 27.4, 25.0. **ESI-MS** (CH_2Cl_2, 180 °C, 3 kV) positive ion: 189.6361 m/z, $[M]^{2+}$ (*calc.* 189.6362). **Anal.** Calcd for $C_{23}H_{33}N_5Br_2$ (539.35 g mol^{-1}): C, 51.22; H, 6.17; N, 12.98. Found: C, 51.08; H, 6.08; N, 12.89.

2c: following the general procedure using 2,6-bis(bromomethyl)pyridine (1.08 g, 4.08 mmol) and **1c** (1.23 g, 4.08 mmol), the product was obtained a white crystalline solid. Yield: 0.90 g (39%).

^{1}H NMR (400 MHz, CD_2Cl_2) δ 10.84 (br, 2H), 8.17 (app. t, J = 2, 2H), 7.69–7.78 (m, 3H), 7.37 (app. t, J = 2, 2H), 5.78 (s, 4H), 4.42 (t, $^3J_{HH}$ = 7.0, 4H), 1.93 (app. pentet, J = 7, 2H), 1.22–1.41 (m, 16H). **^{13}C{^{1}H} NMR** (101 MHz, CD_2Cl_2) δ 153.8, 139.4, 138.4, 124.3, 123.9, 122.0, 53.9, 50.2, 30.0, 28.1 (2C), 27.9, 25.3. **ESI-MS** (CH_2Cl_2, 180 °C, 3 kV) positive ion: 203.6521 m/z, $[M]^{2+}$ (*calc.* 203.6519). **Anal.** Calcd for $C_{25}H_{37}N_5Br_2$ (567.40 g mol^{-1}): C, 52.92; H, 6.57; N, 12.34. Found: C, 52.82; H, 6.53; N, 12.17.

Preparation of [PdCl{CNC-(CH$_2$)$_n$}][BAr$^F_4$] (3)

General procedure. A mixture of **2** (1 equiv.), Ag_2O (1 equiv.) and Na[BAr$^F_4$] (1.1 equiv.) in CH_2Cl_2 (3 mL) were stirred in the absence of light for 16 hours. A solution of $[PdCl_2(NCPh)_2]$ (1 equiv.) in CH_2Cl_2 (*ca.* 3 mL) was added and the suspension stirred for a further 5 hours. The solution was filtered and the filtrate reduced to dryness *in vacuo* to afford the crude product. Purification was achieved by passing through a silica pad using CH_2Cl_2 eluent.

3a: following the general procedure using **2a** (0.060 g, 0.117 mmol) and subsequent recrystallisation from $CHCl_3$–pentane, the product was obtained as pale-yellow crystalline solid. Yield: 0.049 g (31%).

^{1}H NMR (400 MHz, $CDCl_3$) δ 7.71 (t, $^3J_{HH}$ = 7.7, 1H, py), 7.66–7.71 (m, 8H, Ar^F), 7.49 (br, 4H, Ar^F), 7.38 (d, $^3J_{HH}$ = 7.7, 2H, py), 6.94 (d, $^3J_{HH}$ = 1.9, 2H, imid), 6.90 (d, $^3J_{HH}$ = 1.9, 2H, imid), 5.39–5.51 (m, 2H, *N*-CH$_2$), 5.34 (d, $^2J_{HH}$ = 15.3, 2H, py*CH*$_2$), 5.08 (d, $^2J_{HH}$ = 15.3, 2H, py*CH*$_2$), 3.80 (dt, $^2J_{HH}$ = 13.3, $^3J_{HH}$ = 6.6, 2H, *N*-CH$_2$), 2.79 (br, 2H, CH$_2$), 1.98–2.14 (m, 2H, CH$_2$), 1.72–1.86 (m, 2H, CH$_2$), 1.60–1.72 (m, 2H, CH$_2$), 1.41–1.54 (m, 2H, CH$_2$), 1.12–1.25 (m, 2H, CH$_2$). **^{13}C{^{1}H} NMR** (101 MHz, $CDCl_3$) δ 162.4 (s, Pd-C), 161.8 (q, $^1J_{CB}$ = 50, Ar^F), 154.7 (s, py), 141.7 (s, py), 134.9 (s, Ar^F), 129.1 (qq, $^2J_{FC}$ = 32, $^3J_{CB}$ = 3, Ar^F), 125.7 (s, py), 124.6 (q, $^1J_{FC}$ = 273, Ar^F), 123.7 (s, imid), 120.4 (s, imid), 117.7 (pentet, $^3J_{FC}$ = 4, Ar^F), 56.2 (s, py*C*H$_2$), 50.0 (s, *N*-CH$_2$), 31.1 (s, CH$_2$), 26.6 (s, CH$_2$), 26.5 (s, CH$_2$). **ESI-MS** (CH_3CN, 180 °C, 3 kV) positive ion: 490.0993 m/z, $[M]^+$ (*calc*. 490.0989). **Anal.** Calcd for $C_{53}H_{39}BClF_{24}N_5Pd$ (1354.56 g mol^{-1}): C, 46.99; H, 2.90; N, 5.17. Found: C, 46.92; H, 2.87; N, 5.15.

3b: following the general procedure using **2b** (0.064 g, 0.110 mmol) and subsequent recrystallization from $CHCl_3$–pentane, the product was obtained as pale-yellow hexagonal platelets. Yield: 0.094 g (55%).

^{1}H NMR (400 MHz, $CDCl_3$) δ 7.66–7.71 (m, 8H, Ar^F), 7.64 (t, $^3J_{HH}$ = 7.4, 1H, py), 7.49 (br, 4H, Ar^F), 7.35 (d, $^3J_{HH}$ = 7.4, 2H, py), 6.97 (d, $^3J_{HH}$ = 1.7, 2H, imid), 6.87 (d, $^3J_{HH}$ = 1.7, 2H, imid), 5.57 (d, $^3J_{HH}$ = 15.3, 2H, py*CH*$_2$), 4.98 (d, $^3J_{HH}$ = 15.3, 2H, py*CH*$_2$), 4.59–4.73 (m, 2H, *N*-CH$_2$), 4.33–4.46 (m, 2H, *N*-CH$_2$), 2.30–2.43 (m, 2H, CH$_2$), 1.77–1.92 (m, 2H, CH$_2$), 1.57–1.70 (m, 2H, CH$_2$), 1.08–1.48 (m, 10H, CH$_2$). **^{13}C{^{1}H} NMR** (101 MHz, $CDCl_3$) δ 163.3 (s, Pd-C), 161.8 (q, $^1J_{CB}$ = 50, Ar^F), 155.0 (s, py), 141.6 (s, py), 134.9 (s, Ar^F), 129.1 (qq, $^2J_{FC}$ = 32, $^3J_{CB}$ = 3, Ar^F), 125.3 (s, py), 124.6 (q, $^1J_{FC}$ = 273, Ar^F), 123.2 (s, imid), 120.4 (s, imid), 117.7 (pentet, $^3J_{FC}$ = 4, Ar^F), 56.0 (s, py*C*H$_2$), 49.9 (s, *N*-*C*H$_2$), 30.3 (s, CH$_2$), 27.8 (s, CH$_2$), 27.4 (s, CH$_2$), 25.5 (s, CH$_2$). **ESI-MS** (CH_3CN, 180 °C, 3 kV) positive ion: 518.1308 m/z, $[M]^+$ (*calc.* 518.1303). **Anal:** Calcd for $C_{55}H_{43}BClF_{24}N_5Pd$ (1382.61 g mol^{-1}): C, 47.78; H, 3.13; N, 5.07. Found: C, 47.85; H, 3.11; N, 5.07.

3c: following the general procedure using **2c** (0.100 g, 0.176 mmol) and subsequent recrystallization from Et_2O–hexane, the product was obtained as a white crystalline solid. Yield: 0.151 g (58%).

^{1}H NMR (400 MHz, $CDCl_3$) δ 7.66–7.70 (m, 8H, Ar^F), 7.58 (t, $^3J_{HH}$ = 7.6, 1H, py), 7.48 (br, 4H, Ar^F), 7.32 (d, $^3J_{HH}$ = 7.6, 2H, py), 7.02 (d, $^3J_{HH}$ = 1.7, 2H, imid), 6.89 (d, $^3J_{HH}$ = 1.7, 2H, imid), 5.63 (d, $^2J_{HH}$ = 15.0, 2H, py*CH*$_2$), 4.97 (d, $^2J_{HH}$ = 15.0, 2H, py*CH*$_2$), 4.72 (td, J_{HH} = 12.4, $^3J_{HH}$ = 3.6, 2H, *N*-CH$_2$), 3.75 (td, J_{HH} = 12.4, $^3J_{HH}$ = 5.7, 2H, *N*-CH$_2$), 2.09–2.22 (m, 2H, CH$_2$), 1.64–1.77 (m, 2H, CH$_2$), 1.31–1.57 (m, 14H, CH$_2$), 1.08–1.20 (m, 2H, CH$_2$). **^{13}C{^{1}H} NMR** (101 MHz, $CDCl_3$) δ 164.5 (s, Pd-C), 161.8 (q, $^1J_{CB}$ = 50, Ar^F), 154.8 (s, py), 141.5 (s, py), 134.9 (s, Ar^F), 129.1 (qq, $^2J_{FC}$ = 32, $^3J_{CB}$ = 3, Ar^F), 125.4 (s, py), 124.6 (q, $^1J_{FC}$ = 273, Ar^F), 122.4 (s, imid), 121.0 (s, imid), 117.7 (pentet, $^3J_{FC}$ = 4, Ar^F), 55.7 (s, py*C*H$_2$), 51.6 (s, *N*-*C*H$_2$), 31.0 (s, CH$_2$), 28.3 (s, CH$_2$), 27.1 (s, CH$_2$), 27.0 (s, CH$_2$), 23.2 (s, CH$_2$). **ESI-MS** (CH_3CN, 180 °C, 3 kV) positive ion: 546.1616 m/z, $[M]^+$ (*calc.* 546.1617). **Anal.** Calcd for $C_{57}H_{47}BClF_{24}N_5Pd$ (1410.66 g mol^{-1}); C, 48.53; H, 3.36; N, 4.96. Found: C, 48.41; H, 3.29; N, 4.98.

Preparation of [PdF{CNC–$(CH_2)_n$}][$BAr^F{}_4$] (4)

General procedure. To a solution of AgF in MeCN (3 mL) was added a solution of **3** in MeCN (2 mL). The resulting suspension was stirred in the dark at room temperature for 1–3 hours. The solvent was removed *in vacuo* and the product extracted with $CHCl_3$ through celite (Pasteur pipette, 3 cm).

4a: following the general procedure using AgF (0.023 g, 0.181 mmol) and **3a** (0.050 g, 0.037 mmol) – stirred for 1 hour, the product was obtained as an off-white solid. Yield: 0.030 g (61%).

^{1}H NMR (400 MHz, $CDCl_3$) δ 7.67–7.72 (m, 9H, py + Ar^F), 7.49 (br, 4H, Ar^F), 7.35 (d, $^3J_{HH}$ = 7.8, 2H, py), 6.95 (d, $^3J_{HH}$ = 1.8, 2H, imid), 6.90 (d, $^3J_{HH}$ = 1.8, 2H, imid), 5.23 (s, 4H, pyCH_2), 4.31 (app. t, J_{HH} = 7, 4H, *N*-CH_2), 2.04–2.15 (m, 4H, CH_2), 1.42–1.53 (s, 8H, CH_2). **^{19}F NMR** (377 MHz, $CDCl_3$) δ −62.38 (s, Ar^F), −392.08 (s, Pd-F). **^{13}C{^{1}H} NMR** (101 MHz, $CDCl_3$) δ 164.8 (s, Pd-C), 161.8 (q, $^1J_{CB}$ = 50, Ar^F), 155.4 (s, py), 141.2 (s, py), 134.9 (s, Ar^F), 129.1 (qq, $^2J_{FC}$ = 32, $^3J_{CB}$ = 3, Ar^F), 126.2 (s, py), 124.6 (q, $^1J_{FC}$ = 273, Ar^F), 123.2 (s, imid), 119.7 (s, imid), 117.7 (pentet, $^3J_{FC}$ = 4, Ar^F), 55.8 (s, pyCH_2), 50.0 (d, $^{2h}J_{FC}$ = 14, *N*-CH_2), 30.2 (s, CH_2), 26.0 (s, CH_2), 25.5 (d, $^{2h}J_{FC}$ = 6, CH_2). **ESI-MS** (CH_2Cl_2, 180 °C, 3 kV) positive ion: 500.1283 *m*/*z* (100%), $[M - F]^{2+}[HCOO]^-$ (*calc.* 500.1278); 456.1377 *m*/*z* (35%), $[M - F]^{2+}H^-$ (*calc.* 456.1382). **Anal.** Calcd for $C_{53}H_{39}BClF_{25}N_5Pd{\cdot}0.5(CHCl_3)$ (1397.79 [1338.10] g mol^{-1}): C, 45.97; H, 2.85; N, 5.01. Found: C, 45.77; H, 2.86; N, 4.93.

4b: following the general procedure using AgF (0.019 g, 0.150 mmol) and **3b** (0.056 g, 0.041 mmol) – stirred for 3 hours, the product was obtained as a white solid (0.049 g, 88%).

^{1}H NMR (400 MHz, $CDCl_3$) δ 7.67–7.71 (m, 8H, Ar^F), 7.66 (t, $^3J_{HH}$ = 7.8, 1H, py), 7.49 (br, 4H, Ar^F), 7.35 (d, $^3J_{HH}$ = 7.8, 2H, py), 6.98 (d, $^3J_{HH}$ = 1.8, 2H, imid), 6.90 (d, $^3J_{HH}$ = 1.8, 2H, imid), 5.60 (d, $^2J_{HH}$ = 15.2, 2H, pyCH_2), 4.97 (d, $^2J_{HH}$ = 15.2, 2H, pyCH_2), 4.66 (td, J_{HH} = 12.5, $^3J_{HH}$ = 3.9, 2H, *N*-CH_2), 3.71 (td, J_{HH} = 12.5, $^3J_{HH}$ = 5, 2H, *N*-CH_2), 2.00–2.15 (m, 2H, CH_2), 1.34–1.81 (m, 12H, CH_2), 0.97–1.12 (m, 2H, CH_2). **^{19}F NMR** (377 MHz, $CDCl_3$) δ −62.38 (s, Ar^F), −399.89 (s, Pd-F). **^{13}C{^{1}H} NMR** (101 MHz, $CDCl_3$) δ 165.0 (s, Pd-C), 161.8 (q, $^1J_{CB}$ = 50, Ar^F), 155.6 (s, py), 141.2 (s, py), 134.9 (s, Ar^F), 129.1 (qq, $^2J_{FC}$ = 32, $^3J_{CB}$ = 3, Ar^F), 126.0 (s, py), 124.6 (q, $^1J_{FC}$ = 273, Ar^F), 122.3 (s, imid), 120.3 (s, imid), 117.7 (pentet, $^3J_{FC}$ = 4, Ar^F), 55.6 (s, pyCH_2), 50.6 (d, $^{2h}J_{FC}$ = 6, *N*-CH_2), 30.4 (s, CH_2), 27.0 (s, CH_2), 25.6 (s, CH_2), 24.5 (s, CH_2). **ESI-MS** (CH_2Cl_2, 180 °C, 3 kV) positive ion: 542.1762 *m*/*z* (100%), $[M - F]^{2+}[CH_3COO]^-$ (*calc.* 542.1747); 528.1604 *m*/*z* (10%), $[M - F]^{2+}[HCOO]^-$ (*calc.* 528.1591). **Anal.** Calcd for $C_{55}H_{43}BClF_{25}N_5Pd$ (1366.15 g mol^{-1}): C, 48.35; H, 3.17; N, 5.13. Found: C, 48.45; H, 3.11; N, 5.17.

4c: following the general procedure using AgF (0.022 g, 0.173 mmol) and **3c** (0.050 g, 0.035 mmol) – stirred for 1 hour, the product was obtained as an oil that was washed with pentane and dried to give a white foam (0.022 g, 45%).

Table 3 Crystallographic data for **2b**, **3**, **4a** and **4b**

	2b·MeCN	**3a**	**3b**·0.5(pentane)	**3c**·(OEt_2)	**4a**	**4b**
CCDC	961289	961290	961291	961292	961293	961294
Figure	S-31	3	3/SI-32	3	SI-33 + 34	5
Formula	$C_{25}H_{36}Br_2N_6$	$C_{53}H_{39}BClF_{24}N_5Pd$	$C_{57.5}H_{49}BClF_{24}N_5Pd$	$C_{61}H_{57}BClF_{24}N_5OPd$	$C_{53}H_{39}BF_{25}N_5Pd$	$C_{55}H_{43}BF_{25}N_5Pd$
M	580.42	1354.55	1418.67	1484.77	1338.10	1366.15
Crystal system	Monoclinic	Triclinic	Monoclinic	Orthorhombic	Triclinic	Monoclinic
Space group	$P2_1$	$P\bar{1}$	$P2_1/c$	$P2_12_12_1$	$P\bar{1}$	$C2/c$
T [K]	150(2)	150(2)	150(2)	150(2)	150(2)	150(2)
a [Å]	8.6112(4)	13.8039(3)	12.92329(18)	9.7194(4)	12.7226(2)	35.3011(14)
b [Å]	36.1437(11)	14.2173(3)	25.0749(3)	15.1274(5)	18.5028(3)	16.1372(3)
c [Å]	8.7973(3)	15.6408(3)	19.5371(2)	43.507(2)	25.0641(5)	27.1414(11)
α [°]	90	93.0635(17)	90	90	83.7891(16)	90
β [°]	91.596(4)	102.8239(17)	108.9205(15)	90	78.0669(17)	133.337(7)
γ [°]	90	110.5834(19)	90	90	82.1611(16)	90
V [Å^3]	2737.01(17)	2772.73(10)	5988.95(13)	6396.7(5)	5699.2(2)	11 245.5(12)
Z (*Z*′)	4 (2)	2	4	4	4 (2)	8
Density [g cm^{-3}]	1.409	1.622	1.573	1.542	1.559	1.614
μ (mm^{-1})	2.985	0.506	0.472	0.447	0.448	0.456
θ range [°]	$3.2 \le \theta \le 25.0$	$2.9 \le \theta \le 29.6$	$3.0 \le \theta \le 27.9$	$3.1 \le \theta \le 25.0$	$2.9 \le \theta \le 25.7$	$2.9 \le \theta \le 27.9$
Reflns collected	19 071	78 258	88 555	28 972	50 701	34 662
R_{int}	0.0327	0.0360	0.0292	0.0820	0.0325	0.0319
Completeness	99.8	99.9%	99.9%	99.7	99.8	99.8
No. of data/restr/param	9360/223/619	15 538/605/850	14 249/964/968	11 264/753/934	21 631/3975/2076	13 379/710/836
R_1 [$I > 2\sigma(I)$]	0.0495	0.0358	0.0392	0.0937	0.0720	0.0412
wR_2 [all data]	0.1238	0.0862	0.0975	0.2105	0.1988	0.0988
GoF	1.101	1.021	1.058	0.2105	1.022	1.016
Largest diff. pk and hole [e Å^{-3}]	1.52/−0.47	0.82/−0.56	1.03/−0.57	2.11/−1.24	2.60/−1.27	0.93/−0.75
Flack (*x*)	0.024(15)			0.47(7)		

^{1}H NMR (400 MHz, $CDCl_3$) δ 7.64–7.72 (m, 8H, Ar^F), 7.56 (t, $^3J_{HH}$ = 7.7, 1H, py), 7.48 (br, 4H, Ar^F), 7.29 (d, $^3J_{HH}$ = 7.7, 2H, py), 7.01 (d, $^3J_{HH}$ = 1.9, 2H, imid), 6.92 (d, $^3J_{HH}$ = 1.9, 2H, imid), 5.67 (d, $^2J_{HH}$ = 15.1, 2H, pyCH_2), 4.94 (d, $^2J_{HH}$ = 15.1, 2H, pyCH_2), 4.75 (dt, J_{HH} = 12.1, $^3J_{HH}$ = 5.2, 2H, *N*-CH_2), 3.83 (dt, J_{HH} = 11.8, $^3J_{HH}$ = 5.2, 2H, *N*-CH_2), 1.73–1.97 (m, 4H, CH_2), 1.15–1.53 (m, 16H, CH_2). **^{19}F NMR** (377 MHz, $CDCl_3$) δ −62.39 (s, Ar^F), −399.91 (s, Pd-F). **^{13}C{^{1}H} NMR** (101 MHz, $CDCl_3$) δ 164.7 (s, Pd-C), 161.9 (q, $^1J_{CB}$ = 50, Ar^F), 155.8 (s, py), 141.3 (s, py), 134.9 (s, Ar^F), 129.1 (qq, $^2J_{FC}$ = 32, $^3J_{CB}$ = 3, Ar^F), 125.8 (s, py), 124.6 (q, $^1J_{FC}$ = 273, Ar^F), 121.7 (s, imid), 120.6 (s, imid), 117.6 (pentet, $^3J_{FC}$ = 4, Ar^F), 55.6 (s, pyCH_2), 50.0 (d, $^{2h}J_{FC}$ = 6, *N*-CH_2), 31.0 (s, CH_2), 27.4 (s, CH_2), 27.3 (s, CH_2), 27.2 (s, CH_2), 24.4 (s, CH_2). **ESI-MS** (CH_2Cl_2, 180 °C, 3 kV) positive ion: 570.2068 *m*/*z* (100%), $[M - F]^{2+}[CH_3COO]^-$ (*calc.* 570.2060); 556.1902 *m*/*z* (5%), $[M - F]^{2+}[HCOO]^-$ (*calc.* 556.1903). **Anal.** Calcd for $C_{57}H_{47}BClF_{25}N_5Pd$ (1394.21 g mol^{-1}): C, 49.10; H, 3.40; N, 5.02. Found: C, 49.10; H, 3.28; N, 5.13.

Variable temperature NMR experiments

All measurements were performed using a DRX-500 spectrometer. Samples (0.014 M in CD_2Cl_2) were prepared in J. Youngs NMR tubes under inert atmosphere and equilibrated at each temperature inside the spectrometer for 10 minutes prior to data acquisition. Spectra and selected data are compiled in the ESI.†

Crystallography

Crystallographic data for **2b**, **3** and **4** are summarised in Table 3. Full details about the collection, solution and refinement are documented in the CIF, which have been deposited with the Cambridge Crystallographic Data Centre under CCDC 961289–961294.

Acknowledgements

We thank the University of Warwick (R.E.A.) and the Royal Society (A.B.C.) for financial support.

References

1 (*a*) S. Díez-González, N. Marion and S. P. Nolan, *Chem. Rev.*, 2009, **109**, 3612–3676; (*b*) C. Samojłowicz, M. Bieniek and K. Grela, *Chem. Rev.*, 2009, **109**, 3708–3742; (*c*) F. E. Hahn and M. C. Jahnke, *Angew. Chem., Int. Ed.*, 2008, **47**, 3122–3172; (*d*) S. Würtz and F. Glorius, *Acc. Chem. Res.*, 2008, **41**, 1523–1533.

2 M. Poyatos, J. A. Mata and E. Peris, *Chem. Rev.*, 2009, **109**, 3677–3707.

3 (*a*) P. G. Edwards and F. E. Hahn, *Dalton Trans.*, 2011, **40**, 10278–10288; (*b*) L. Benhamou, E. Chardon, G. Lavigne, S. Bellemin-Laponnaz and V. Cesar, *Chem. Rev.*, 2011, **111**, 2705–2733.

4 (*a*) M. Albrecht and M. M. Lindner, *Dalton Trans.*, 2011, **40**, 8733–8744; (*b*) J. Choi, A. H. R. MacArthur, M. Brookhart and A. S. Goldman, *Chem. Rev.*, 2011, **111**, 1761–1779; (*c*) W. H. Bernskoetter, C. K. Schauer, K. I. Goldberg and M. Brookhart, *Science*, 2009, **326**, 553–556; (*d*) M. E. van der Boom and D. Milstein, *Chem. Rev.*, 2003, **103**, 1759–1792; (*e*) M. Albrecht and G. van Koten, *Angew. Chem., Int. Ed.*, 2001, **40**, 3750–3781.

5 (*a*) J. A. Mata, M. Poyatos and E. Peris, *Coord. Chem. Rev.*, 2007, **251**, 841–859; (*b*) D. Pugh and A. A. Danopoulos, *Coord. Chem. Rev.*, 2007, **251**, 610–641; (*c*) E. Peris and R. H. Crabtree, *Coord. Chem. Rev.*, 2004, **248**, 2239–2246.

6 For representative examples see: (*a*) T. R. Helgert, T. K. Hollis and E. J. Valente, *Organometallics*, 2012, **31**, 3002–3009; (*b*) X. Zhang, A. M. Wright, N. J. DeYonker, T. K. Hollis, N. I. Hammer, C. E. Webster and E. J. Valente, *Organometallics*, 2012, **31**, 1664–1672; (*c*) D. Serra, P. Cao, J. Cabrera, R. Padilla, F. Rominger and M. Limbach, *Organometallics*, 2011, **30**, 1885–1895; (*d*) K. M. Schultz, K. I. Goldberg, D. G. Gusev and D. M. Heinekey, *Organometallics*, 2011, **30**, 1429–1437; (*e*) K. Inamoto, J.-I. Kuroda, E. Kwon, K. Hiroya and T. Doi, *J. Organomet. Chem.*, 2009, **694**, 389–396; (*f*) A. A. Danopoulos, D. Pugh and J. A. Wright, *Angew. Chem., Int. Ed.*, 2008, **47**, 9765–9767; (*g*) J. A. Wright, A. A. Danopoulos, W. B. Motherwell, R. J. Carroll, S. Ellwood and J. Saßmannshausen, *Chem. Ber.*, 2006, **2006**, 4857–4865; (*h*) A. A. Danopoulos, J. A. Wright, W. B. Motherwell and S. Ellwood, *Organometallics*, 2004, **23**, 4807–4810.

7 (*a*) C. Gao, H. Zhou, S. Wei, Y. Zhao, J. You and G. Gao, *Chem. Commun.*, 2013, **49**, 1127–1129; (*b*) F. E. Hahn, M. C. Jahnke and T. Pape, *Organometallics*, 2007, **26**, 150–154; (*c*) F. E. Hahn, M. C. Jahnke, V. Gomez-Benitez, D. Morales-Morales and T. Pape, *Organometallics*, 2005, **24**, 6458–6463; (*d*) M. Poyatos, F. Márquez, E. Peris, C. Claver and E. Fernandez, *New J. Chem.*, 2002, **27**, 425–431; (*e*) J. A. Loch, M. Albrecht, E. Peris, J. Mata, J. W. Faller and R. H. Crabtree, *Organometallics*, 2002, **21**, 700–706; (*f*) E. Peris, J. Mata, J. A. Loch and R. H. Crabtree, *Chem. Commun.*, 2001, 201–202.

8 A. A. D. Tulloch, A. A. Danopoulos, G. J. Tizzard, S. J. Coles, M. B. Hursthouse, R. S. Hay-Motherwell and W. B. Motherwell, *Chem. Commun.*, 2001, 1270–1271.

9 A. A. Danopoulos, A. A. D. Tulloch, S. Winston, G. Eastham and M. B. Hursthouse, *Dalton Trans.*, 2003, 1009–1015.

10 D. J. Nielsen, K. J. Cavell, B. W. Skelton and A. H. White, *Inorg. Chim. Acta*, 2006, **359**, 1855–1869.

11 R. S. Simons, P. Custer, C. A. Tessier and W. J. Youngs, *Organometallics*, 2003, **22**, 1979–1982.

12 J. R. Miecznikowski, S. Gründemann, M. Albrecht, C. Mégret, E. Clot, J. W. Faller, O. Eisenstein and R. H. Crabtree, *Dalton Trans.*, 2003, 831–838.

13 D. J. Nielsen, K. J. Cavell, B. W. Skelton and A. H. White, *Inorg. Chim. Acta*, 2002, **327**, 116–125.

14 S. Gründemann, M. Albrecht, J. A. Loch, J. W. Faller and R. H. Crabtree, *Organometallics*, 2001, **20**, 5485–5488.

15 (*a*) X. Zhang, D. Huang, Y.-S. Chen and R. H. Holm, *Inorg. Chem.*, 2012, **51**, 11017–11029; (*b*) J. Kickham, S. Loeb and S. Murphy, *Chem.–Eur. J.*, 1997, **3**, 1203–1213; (*c*) B. R. Cameron, S. J. Loeb and G. P. A. Yap, *Inorg. Chem.*, 1997, **36**, 5498–5504; (*d*) J. Kickham and S. Loeb, *Inorg. Chem.*, 1995, **34**, 5656–5665; (*e*) J. Kickham and S. Loeb, *Inorg. Chem.*, 1994, **33**, 4351–4359; (*f*) J. Kickham, S. Loeb and S. Murphy, *J. Am. Chem. Soc.*, 1993, **115**, 7031–7032.

16 (*a*) G. De Bo, J. De Winter, P. Gerbaux and C.-A. Fustin, *Angew. Chem., Int. Ed.*, 2011, **50**, 9093–9096; (*b*) S. M. Goldup, D. A. Leigh, R. T. McBurney, P. R. McGonigal and A. Plant, *Chem. Sci.*, 2010, **1**, 383; (*c*) S. M. Goldup, D. A. Leigh, P. J. Lusby, R. T. McBurney and A. M. Z. Slawin, *Angew. Chem., Int. Ed.*, 2008, **47**, 3381–3384; (*d*) V. Aucagne, J. Berná, J. D. Crowley, S. M. Goldup, K. D. Hänni, D. A. Leigh, P. J. Lusby, V. E. Ronaldson, A. M. Z. Slawin, A. Viterisi and D. B. Walker, *J. Am. Chem. Soc.*, 2007, **129**, 11950–11963; (*e*) L. Hogg, D. A. Leigh, P. J. Lusby, A. Morelli, S. Parsons and J. K. Y. Wong, *Angew. Chem., Int. Ed.*, 2004, **43**, 1218–1221.

17 Such species have notably found application in anion sensing: (*a*) H.-Y. Gong, B. M. Rambo, V. M. Lynch, K. M. Keller and J. L. Sessler, *J. Am. Chem. Soc.*, 2013, **135**, 6330–6337; (*b*) H.-T. Niu, Z. Yin, D. Su, D. Niu, Y. Ao, J. He and J.-P. Cheng, *Tetrahedron*, 2008, **64**, 6300–6306; (*c*) V. K. Khatri, M. Chahar, K. Pavani and P. S. Pandey, *J. Org. Chem.*, 2007, **72**, 10224–10226; (*d*) J. Yoon, S. K. Kim, N. J. Singh and K. S. Kim, *Chem. Soc. Rev.*, 2006, **35**, 355; (*e*) M. V. Baker, M. J. Bosnich, D. H. Brown, L. T. Byrne, V. J. Hesler, B. W. Skelton, A. H. White and C. C. Williams, *J. Org. Chem.*, 2004, **69**, 7640–7652.

18 C. Radloff, H.-Y. Gong, C. Schulte to Brinke, T. Pape, V. M. Lynch, J. L. Sessler and F. E. Hahn, *Chem.–Eur. J.*, 2010, **16**, 13077–13081.

19 A range of pyridine based bis-NHC cyclophanes complexes are known, although they adopt dinuclear coordination geometries: (*a*) M. V. Baker, D. H. Brown, R. A. Haque, P. V. Simpson, B. W. Skelton, A. H. White and C. C. Williams, *Organometallics*, 2009, **28**, 3793–3803; (*b*) A. Melaiye, Z. Sun, K. Hindi, A. Milsted, D. Ely, D. H. Reneker, C. A. Tessier and W. J. Youngs, *J. Am. Chem. Soc.*, 2005, **127**, 2285–2291; (*c*) P. J. Barnard, M. V. Baker, S. J. Berners-Price, B. W. Skelton and A. H. White, *Dalton Trans.*, 2004, 1038; (*d*) J. C. Garrison, R. S. Simons, J. M. Talley, C. Wesdemiotis, C. A. Tessier and W. J. Youngs, *Organometallics*, 2001, **20**, 1276–1278; (*e*) J. C. Garrison, R. S. Simons, W. G. Kofron, C. A. Tessier and W. J. Youngs, *Chem. Commun.*, 2001, 1780–1781. For a unique exception see: M. V. Baker, B. W. Skelton, A. H. White and C. C. Williams, *Organometallics*, 2002, **21**, 2674–2678.

20 S. Saito, I. Azumaya, N. Watarai, H. Kawasaki and R. Yamasaki, *Heterocycles*, 2009, **79**, 531–548.

21 K. Meyer, A. F. Dalebrook and L. J. Wright, *Dalton Trans.*, 2012, **41**, 14059–14067.

22 (*a*) M. V. Baker, S. K. Brayshaw, B. W. Skelton, A. H. White and C. C. Williams, *J. Organomet. Chem.*, 2005, **690**, 2312–2322; (*b*) M. V. Baker, B. W. Skelton, A. H. White and C. C. Williams, *J. Chem. Soc., Dalton Trans.*, 2001, 111–120.

23 (*a*) O. Shoji, S. Okada, A. Satake and Y. Kobuke, *J. Am. Chem. Soc.*, 2005, **127**, 2201–2210; (*b*) J. Z. Vlahakis, S. Mitu, G. Roman, E. Patricia Rodriguez, I. E. Crandall and W. A. Szarek, *Bioorg. Med. Chem.*, 2011, **19**, 6525–6542.

24 For example see: (*a*) B. Szyszko, L. Latos-Grazyński and L. Szterenberg, *Angew. Chem., Int. Ed.*, 2011, **50**, 6587–6591; (*b*) P. Štěpnička, H. Solařová and I. Císařová, *J. Organomet. Chem.*, 2011, **696**, 3727–3740; (*c*) M. Bröring and C. Kleeberg, *Z. Anorg. Allg. Chem.*, 2007, **633**, 2210–2216.

25 The conditions under which this coalescence temperature was measured are unclear: either a 400 or 500 MHz spectrometer was used.

26 See for example: (*a*) T. M. Douglas, E. Molinos, S. K. Brayshaw and A. S. Weller, *Organometallics*, 2007, **26**, 463–465; (*b*) I. Krossing and I. Raabe, *Angew. Chem., Int. Ed.*, 2004, **43**, 2066–2090.

27 gNMR (Adept Scientific, Herts, UK), v 4.1.2.

28 W. Kemp, *NMR in Chemistry: A multinuclear introduction*, Macmillan, Hampshire, UK, 1986.

29 (*a*) N. D. Ball, J. W. Kampf and M. S. Sanford, *Dalton Trans.*, 2010, 632–640; (*b*) V. V. Grushin and W. J. Marshall, *J. Am. Chem. Soc.*, 2009, **131**, 918–919; (*c*) D. A. Watson, M. Su, G. Teverovskiy, Y. Zhang, J. García-Fortanet, T. Kinzel and S. L. Buchwald, *Science*, 2009, **325**, 1661–1664; (*d*) N. D. Ball and M. S. Sanford, *J. Am. Chem. Soc.*, 2009, **131**, 3796–3797; (*e*) V. V. Grushin, *Chem.–Eur. J.*, 2002, **8**, 1006–1014; (*f*) M. C. Pilon and V. V. Grushin, *Organometallics*, 1998, **17**, 1774–1781; (*g*) S. L. Fraser, M. Y. Antipin, V. N. Khroustalyov and V. V. Grushin, *J. Am. Chem. Soc.*, 1997, **119**, 4769–4770.

30 (*a*) S. R. Caskey, M. H. Stewart, Y. J. Ahn, M. J. A. Johnson, J. L. C. Rowsell and J. W. Kampf, *Organometallics*, 2007, **26**, 1912–1923; (*b*) C. J. Bourgeois, S. A. Garratt, R. P. Hughes, R. B. Larichev, J. M. Smith, A. J. Ward, S. Willemsen, D. Zhang, A. G. DiPasquale, L. N. Zakharov and A. L. Rheingold, *Organometallics*, 2006, **25**, 3474–3480; (*c*) A. Yahav, I. Goldberg and A. Vigalok, *Inorg. Chem.*, 2005, **44**, 1547–1553; (*d*) J. E. Veltheer, P. Burger and R. G. Bergman, *J. Am. Chem. Soc.*, 1995, **117**, 12478–12488; (*e*) S. K. Agbossou, C. Roger, A. Igau and J. A. Gladysz, *Inorg. Chem.*, 1992, **31**, 419–424; (*f*) S. A. Brewer, J. H. Holloway, E. G. Hope and P. G. Watson, *J. Chem. Soc., Chem. Commun.*, 1992, 1577.

31 R. Huacuja, D. E. Herbert, C. M. Fafard and O. V. Ozerov, *J. Fluorine Chem.*, 2010, **131**, 1257–1261.

32 (*a*) S. C. F. Kui, N. Zhu and M. C. W. Chan, *Angew. Chem., Int. Ed.*, 2003, **42**, 1628–1632; (*b*) D. L. Bryce and R. E. Wasylishen, *J. Mol. Struct.*, 2002, **602**, 463–472; (*c*) G. R. Desiraju, *Acc. Chem. Res.*, 2002, **35**, 565–573;

(*d*) G. W. Gribble, E. R. Olson, J. H. Brown and C. H. Bushweller, *J. Org. Chem.*, 1993, **58**, 1631–1634.
33 Preliminary catalytic data for **3c** (Heck reaction) is detailed in the ESI.†
34 W. E. Buschmann, J. S. Miller, K. Bowman-James and C. N. Miller, *Inorg. Synth.*, 2002, **33**, 83–91.
35 J. A. McCleverty, G. Wilkinson, L. G. Lipson, M. L. Maddox and H. D. Kaesz, *Inorg. Synth.*, 1990, **28**, 84–86.